

Study of Surface Modification of Niobium Caused by Nitriding and Cathodic Cage Deposition

Francisco R. C. Macedo^a, Renan M. Monção^a , José C. A. Queiroz^b, Maxwell S. Libório^{c*} ,
José A. P. Costa^d, Luciana S. Rossino^e, Miguel R. Danelon^e, Michelle C. Feitor^b,
Thércio H. C. Costa^b, Rômulo R. M. Sousa^a 

^aUniversidade Federal do Piauí, Departamento de Engenharia Mecânica, Teresina, PI, Brasil.

^bUniversidade Federal do Rio Grande do Norte, Programa de Pós-graduação em Engenharia Mecânica, Natal, RN, Brasil.

^cUniversidade Federal do Rio Grande do Norte, Escola de Ciências e Tecnologia, Natal, RN, Brasil.

^dUniversidade Estadual do Rio Grande do Norte, Departamento de Física, Mossoró, RN, Brasil.

^eUniversidade Federal de São Carlos, Programa de Pós-graduação em Ciências e Engenharia de Materiais, Sorocaba, SP, Brasil.

Received: December 21, 2022; Revised: March 15, 2023; Accepted: March 30, 2023

In this work, plasma nitriding (PN) and cathode cage plasma deposition (CCPN) treatments were carried out with temperatures of 400 and 450 °C to evaluate the modifications caused on the surface of pure niobium samples. XRD, SEM, Vickers microhardness, and sphere-disk analyses were used to characterize the coatings' composition, morphology, hardness, and wear resistance. The results showed that the treated samples increased hardness and wear resistance, with the sample submitted to CCPN at 450 °C presenting the best tribological behavior.

Keywords: Niobium nitride, nitriding, plasma deposition, wear resistance.

1. Introduction

Brazil has the world's largest deposits of Niobium (Nb), and this metal is strategically important as a target for research to determine different uses and new industrial applications. In recent years, the application of Nb for different uses, such as micro-alloyed steels to promote good weldability and toughness¹⁻³, superalloys⁴, thin films⁵, medical implants⁶, and superconductors, has steadily increasing⁷. Furthermore, this metal does not oxidize at room temperature, and its properties vary depending on the content of interstitial elements⁸.

Nitriding and plasma deposition has been widely used to form niobium nitrides to improve the tribological behavior of several steels. In addition, these nitrides can act as protective layers against oxidation processes⁹ and improve tribological performance¹⁰. Niobium nitride has excellent physical and chemical properties such as hardness¹¹, wear resistance¹², chemical stability¹³, and superconducting properties¹⁴ high electrical conductivity, and superconducting transition temperature^{15,16}. Furthermore, plasma nitriding can form a transition layer produced by nitrogen diffusion on the metal surface. This can reduce tensions resulting from the interface between film and substrate, which results from the contrast between the mechanical properties between the metal and the film deposited on it¹⁷.

Singh et al.¹⁸, in 2012, performed the deposition of NbN films to improve the surface hardness of various steel substrates. This work is related to the formation of hard films composed of phases of the Nb_xN_y type.

Furthermore, the authors varied the nitrogen flow to cause changes in the phases produced in the sputtering process and observed that films composed of Nb₂N had the lowest hardness values among the films produced¹⁸. NbN coatings have been an excellent alternative for improving tribological behavior by showing greater wear resistance than commercially used coatings such as TiN, reports Zhitomirsky¹⁹ in 2007.

In this work, plasma nitriding (PN) and cathodic cage plasma deposition (CCPD) will be performed with temperature variation to produce surface modification by inserting nitrogen on the surface and deposition of a hard and wear-resistant Nb_xN_y composite film featuring better tribological performance and longer functional life of the studied metal. The results obtained should contribute to the discussion about the relevance of using Nb and NbN as functional coatings for application in the metalworking industry.

2. Materials and Methods

This work used cylindrical samples of pure niobium metal (Nb). Those samples were treated with plasma under four different conditions, and your results were compared with samples without treatment. All samples had their upper surfaces prepared with 400 to 1200 mesh sandpaper and polished with diamond paste until a mirrored and scratch-free appearance was acquired. Before the plasma treatment, the samples were dipped in alcohol, subjected to ultrasound for 10 minutes to eliminate remaining impurities, and dried with airflow at room temperature^{20,21}.

*e-mail: maxwellprog@hotmail.com

Table 1. Plasma nitriding treatment parameters.

Samples	PN treatment		CCPD treatment	
	PN400	PN450	CCPD400	CCPD450
Temperature (°C)	400	450	400	450
Gases (sccm)	48 N ₂ / 12 H ₂			
Pressure (Pa)	600	600	200	200
Time (hours)	4	4	4	4

Source: self-authored (2022).

The equipment used for plasma treatments consists of a gas supply system, a reactor, a direct current source with a maximum value of 2 A, a vacuum pump, and a digital thermometer. The whole apparatus is better described in previous works^{21,22}. The treatments were performed with a pre-sputtering stage lasting one hour, 350 °C, and 1:1 flow (Ar/H₂) to remove remaining residues. Soon after, PN or CCPD treatments are effectively started with the parameters shown in Table 1.

A niobium cage of approximately 7.2 cm in diameter, 3.5 cm in height, and 2 mm in thickness was used for the cathodic cage deposition (CCPD) step. An alumina disk was used to keep the samples on fluctuating potential during the depositions.

The phase composition was analyzed using an X-ray diffractogram (XRD) from Shimadzu, model XRD-6000. Cu K α lines (wavelength: 0.154 nm) were used, operating with 40 kV and 30 mA in the range of 30 to 65 ° in the Bragg-Brentano configuration. The scanning electron microscope FEI COMPANY, model QUANTA FEG 250, was used to evaluate the thickness and morphology of the deposited layers. Five thickness measurements were made along the length of the layers to obtain the average values and their standard deviations. The hardness test was carried out using an INSIZE microdurometer, model ISH-TDV 1000. A Vickers indenter (HV) with a load of 50 gf and duration of 15 seconds was used in the test, and five measurements were taken to obtain the hardness value average. The micro-abrasive wear test was performed with ball-disc-type equipment to assess the wear volume of the samples. The SAE 52100 steel ball has a diameter of 25.4 mm, and the tests were carried out with a normal load of 8 N, a rotation frequency of 40 Hz, for 600 s, without lubricant. Three tests were performed on each sample to obtain measurements of the average diameter of the wear trail.

3. Results and Discussion

The X-ray diffraction results of pure niobium and samples submitted to PN and CCPD treatments are shown in Figure 1. Despite the conventional nitriding process, samples PN400 and PN450 did not show Nb_xN_y phases. However, the PN treatments caused diffraction peak displacement due to the insertion of nitrogen in the niobium matrix (Nb - ICSD 76416). According to Kertscher et al.²³, on the solvus curve for the α -Nb(N) phase, the solubility of nitrogen in niobium bcc ranges from < 3 wt% N at a

Table 2. Mean and standard deviation layer thicknesses of samples with conventional nitriding and cathodic cage nitriding.

Samples	Thickness (μ m)	Standard deviation (μ m)
PN400	7.49	0.87
PN450	7.89	0.35
CCPD400	0.82	0.50
CCPD450	8.02	0.51

Source: self-authored (2022).

temperature of \approx 2350 °C to zero at room temperature²³. Therefore, the low amount of nitrogen in the niobium matrix caused peak shifts of little significance. On the other hand, the diffractograms of the samples treated by CCPD showed the formation of phases Nb₄N₅ (ICSD 26251) and Nb₂N (ICSD 76387) that present high hardness and thermodynamic stability, in addition to improving resistance to wear and corrosion²⁴⁻²⁷.

Figure 2 shows the surface electronic microscopy of the Base sample (without treatment). The sample preparation process consisting of sanding and polishing can reduce irregularities. Despite this, the presence of remaining surface imperfections is noted.

The electronic micrographs of the treated samples are shown in Figure 3. The surfaces of the PN400 and PN450 samples were more regular than the surface of the Base sample, except for some areas of discontinuity. This can occur due to irregularities of the pre-treatment surface or possible opening of electrical arcs on the sample during nitriding.

Samples submitted to CCPD treatment showed fewer surface defects due to the deposition of Nb_xN_y films. Figure 3b shows that the film produced by CCPD at 400 °C is very thin, unable to highlight it in the cross-sectional SEM. The surface image of the CCPD400 sample shows the formation of refined grains, which characterizes a low deposition rate under the conditions adopted in the treatment. On the other hand, the CCPD450 sample showed an expressive layer evolution and the formation of larger grains. The increase in temperature caused a higher sputtering rate and more significant deposition of the Nb_xN_y film on the substrate.

Table 2 presents the layer thickness values and their respective standard deviations. As observed in the electron microscopy images, layers were formed by nitriding.

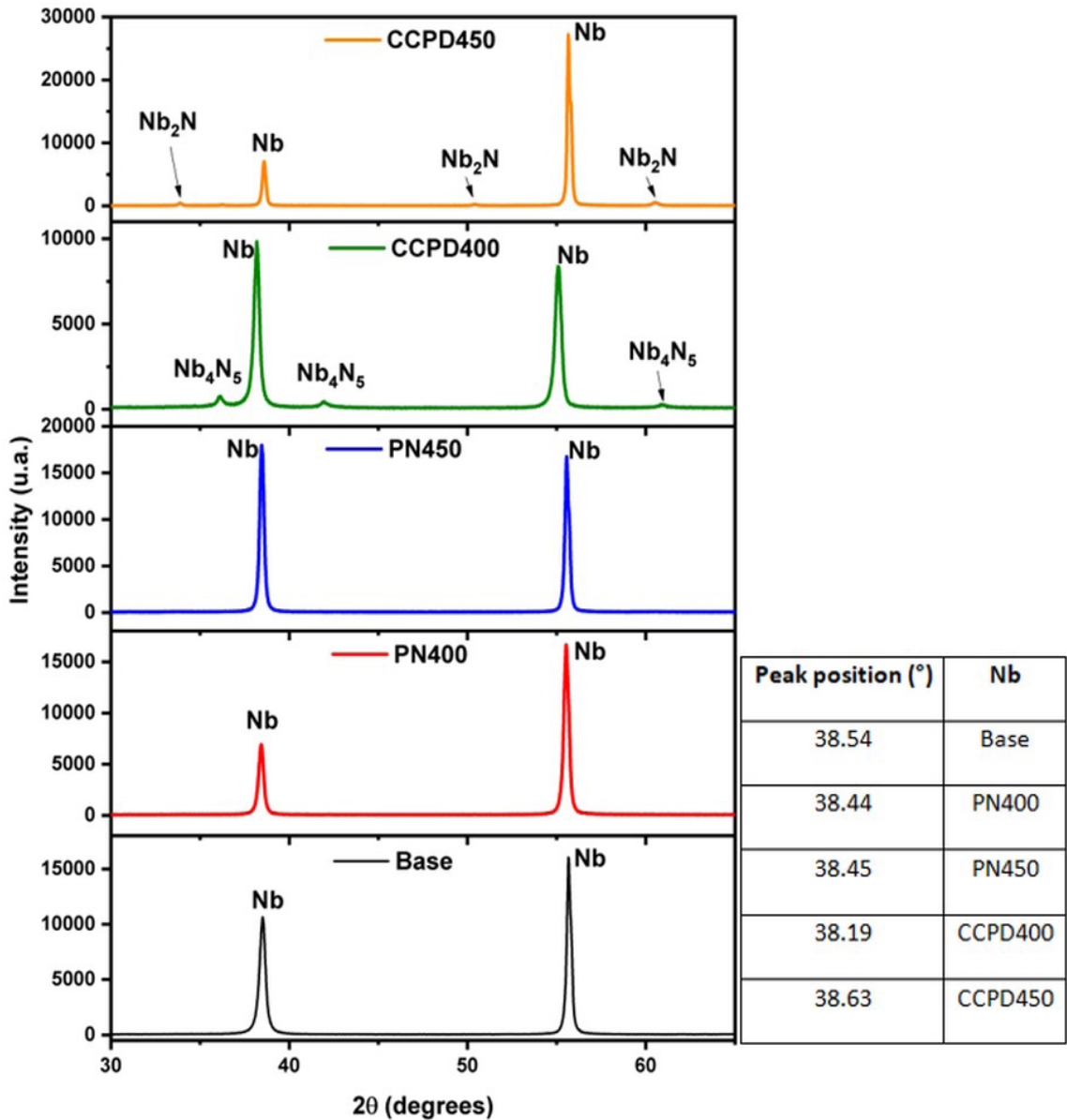


Figure 1. X-ray diffractogram and the 2θ position of the 100% peak.

However, these thick layers are constituted by niobium, with a low content of nitrogen diffused in its structure. The low thickness of the layer formed in the CCPD400 sample shows that under this temperature and pressure condition, it was impossible to promote an efficient deposition rate like that observed in the deposition at 450 °C (CCPD450).

Figure 4 shows the surface hardness values of the nitrided and CCPD-treated samples and compares the treated samples with the base sample (Nb). All samples subjected to plasma treatment showed higher surface hardness than the untreated sample. Samples nitrided at 400 °C and 450 °C obtained hardness values of approximately 279 HV and 245 HV, respectively. The CCPD400 sample showed higher hardness due to the formation of niobium nitride phases, as shown in the x-ray diffractogram in

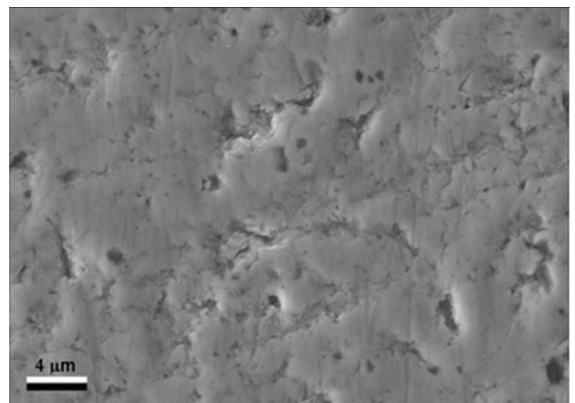


Figure 2. Surface SEM of the Base sample.

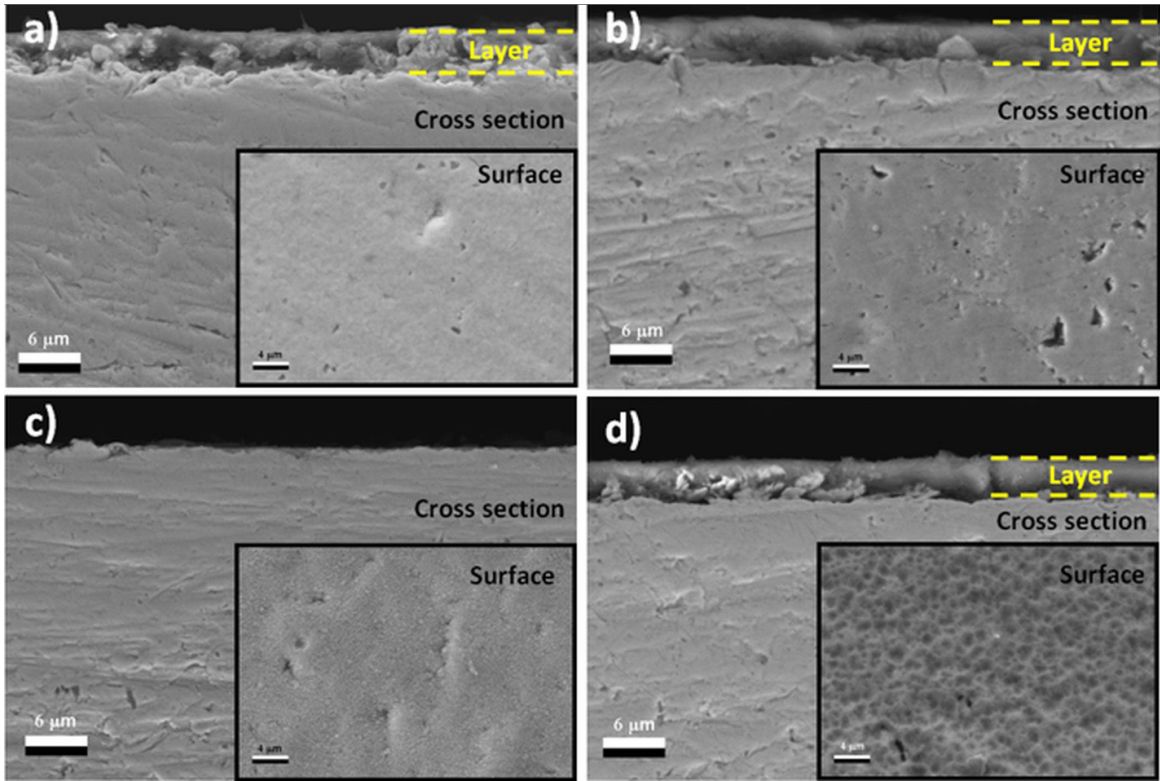


Figure 3. Micrographs obtained by SEM of niobium samples nitrided conventionally and in the cathodic cage. a), b), c), and d), respectively, PN400, PN450, CCPD400, and CCPD450.

Figure 1. Unexpectedly, the surface hardness value of the CCPD450 sample was the lowest among the treated samples. This can be explained by possibly forming a less dense, less resistant film than the layer modified by the deposition treatment at 400 °C.

The optical microscopy images of the trail formed in the sphere-disc wear test are shown in Figure 5. The untreated sample showed a more extensive trail with regions marked by adhesive wear resulting from sliding contact with the sphere used in the tribological test. Conversely, the nitrided samples showed a smaller trail size, characterizing less wear. In these samples, wear by scratching was more evident on the surfaces. On the other hand, the samples submitted to the deposition process showed little wear trail. The CCPD400 sample showed less trail and adhesive wear. Samples with niobium nitride thin films were more wear-resistant than nitrided samples. The Vickers hardness results showed low values for the CCPD450 sample to the nitrided samples. However, the image of the wear trail of this sample showed more excellent resistance in the sliding contact.

Figure 6 shows the wear volumes of the samples submitted to the sphere-disk type tribological test. Plasma-treated samples had less wear volume when compared to the untreated sample. Among the treated samples, PN450 showed the worst average performance. On the other hand, the CCPD450 sample had a smaller wear volume, which characterizes greater resistance to wear than the

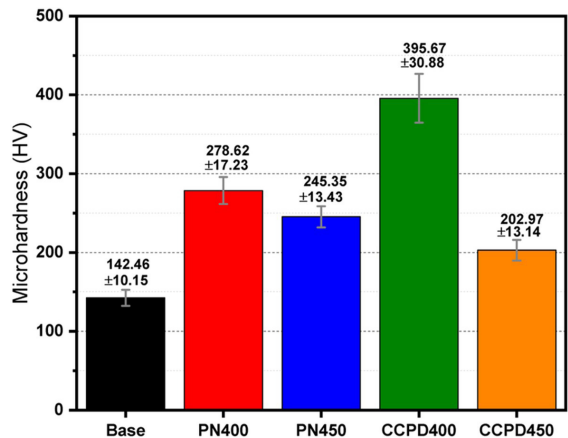


Figure 4. Microhardness values of treated and untreated niobium samples.

sample with niobium nitride film. The PN400 sample also showed behavior comparable to the deposited samples in the tribological test. As seen in Figure 5b, the region of contact between the surfaces in the tribological test was close to surface deformations that may have influenced the accuracy of the numerical result. Despite this, the result for PN400 is close to the values obtained for PN450, considering the standard deviation.

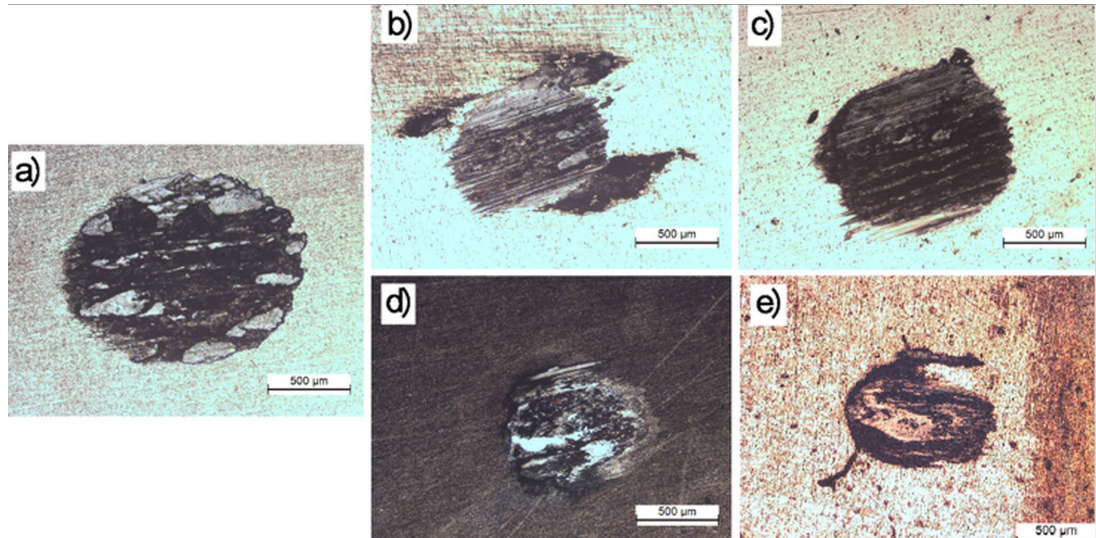


Figure 5. Trail form in the wear test for each sample. a) Base, b) PN400, c) PN450, d) CCPD400, and e) CCPD450.

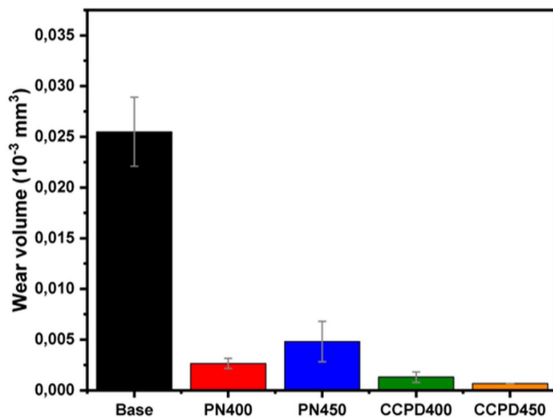


Figure 6. Volume of wear of the samples submitted to the sphere-disk type tribological test.

4. Conclusions

The results obtained in this work allowed the following conclusions:

- The nitriding treatments carried out at 400 °C, and 450 °C showed only Nb phases distorted in the diffractograms by the presence of a small amount of accompaniment in the steel matrix.
- The samples kept in the CCPD treatment showed the formation of the Nb_4N_5 and Nb_2N phases responsible for the hardening of the surface of the samples.
- In the results of scanning electron microscopy also observed the formation of thick layers, except in the CCPD400 sample, which did not present adequate temperature and gas pressure conditions to form niobium nitride phases.
- The wear test showed that the treatments improved wear resistance. In addition, nitriding and deposition of niobium nitrides resulted in the best tribological behavior of the studied steel.

Therefore, the appreciated results that formed a layer composed of Nb with diffusion in nitriding and Nb_xN_y in deposition reduce steel wear in industrial applications.

5. Acknowledgements

This study was financed in part by the Coordenação de Aperfeiçoamento de Pessoal de Nível Superior - Brasil (CAPES) - Finance Code 001.

This study was financed by the Conselho Nacional de Desenvolvimento Científico e Tecnológico – Brasil (CNPq) – Project 08289/2021-8

6. References

1. Anijdan SHM, Sediako D, Yue S. Optimization of flow stress in cool deformed Nb-microalloyed steel by combining strain induced transformation of retained austenite, cooling rate and heat treatment. *Acta Mater.* 2012;60(3):1221-9.
2. Anijdan SHM, Rezaeian A, Yue S. The effect of chemical composition and austenite conditioning on the transformation behavior of microalloyed steels. *Mater Charact.* 2012;63:27-38.
3. Okamoto R, Borgenstam A, Ågren J. Interphase precipitation in niobium-microalloyed steels. *Acta Mater.* 2010;58(14):4783-90.
4. Zhao K, Lou LH, Ma YH, Hu ZQ. Effect of minor niobium addition on microstructure of a nickel-base directionally solidified superalloy. *Mater Sci Eng A.* 2008;476(1-2):372-7.
5. Okolo B, Lamparter P, Welzel U, Mittemeijer EJ. Stress, texture, and microstructure in niobium thin films sputter deposited onto amorphous substrates. *J Appl Phys.* 2004 [cited 2022 Nov 16];95(2):466-76. <https://aip.scitation.org/doi/abs/10.1063/1.1631733>.
6. Johansson CB, Albrektsson T. A removal torque and histomorphometric study of commercially pure niobium and titanium implants in rabbit bone. *Clin Oral Implants Res.* 1991 [cited 2022 Nov 15];2(1):24-9. <https://onlinelibrary.wiley.com/doi/full/10.1034/j.1600-0501.1991.020103.x>.
7. Alves AR, Coutinho AR. Life cycle assessment of niobium: a mining and production case study in Brazil. *Miner Eng.* 2019;132:275-83.
8. Brunatto SF, Allenstein AN, Allenstein CLM, Buschinelli AJA. Cavitation erosion behaviour of niobium. *Wear.* 2012;274-275:220-8.

9. ASM International. ASM handbook volume 5: surface engineering. Materials Park: ASM International.
10. Kertscher R, Brunatto SF. On the kinetics of nitride and diffusion layer growth in niobium plasma nitriding. *Surf Coat Tech.* 2020;401:126220.
11. Ufuktepe Y, Farha AH, Kimura SI, Hajiri T, Karadağ F, Mamun MAA et al. Structural, electronic, and mechanical properties of niobium nitride prepared by thermal diffusion in nitrogen. *Mater Chem Phys.* 2013;141(1):393-400.
12. Melo INR, Silva AE, Faria FG, Pinheiro IP, Silva LR, Paniago RM. Influence of niobium adding on the microstructure and abrasive wear resistance of a heat-treated high-chromium near-eutectic cast iron alloy. *Mater Res.* 2022;25:e20210562. <https://doi.org/10.1590/1980-5373-MR-2021-0562>.
13. Singewald TD, Traxler I, Schimo-Aichhorn G, Hild S, Valtiner M. Versatile, low-cost, non-toxic potentiometric pH-sensors based on niobium. *Sens Biosensing Res.* 2022;35:100478.
14. Oyama ST. The chemistry of transition metal carbides and nitrides. Dordrecht: Springer; 1996. Chapter 1, Introduction to the chemistry of transition metal carbides and nitrides; p. 1-27.
15. Mercier F, Coindeau S, Lay S, Crisci A, Benz M, Encinas T et al. Niobium nitride thin films deposited by high temperature chemical vapor deposition. *Surf Coat Tech.* 2014;260:126-32.
16. Farha AH, Ozkendir OM, Elsayed-Ali HE, Myneni G, Ufuktepe Y. The effect of heat treatment on structural and electronic properties of niobium nitride prepared by a thermal diffusion method. *Surf Coat Tech.* 2017;309:54-8.
17. Pender DC, Padture NP, Giannakopoulos AE, Suresh S. Gradients in elastic modulus for improved contact-damage resistance. Part I: the silicon nitride-oxy-nitride glass system. *Acta Mater.* 2001;49(16):3255-62.
18. Singh K, Krishnamurthy N, Suri AK. Adhesion and wear studies of magnetron sputtered NbN films. *Tribol Int.* 2012;50:16-25.
19. Zhitomirsky VN. Structure and properties of cathodic vacuum arc deposited NbN and NbN-based multi-component and multi-layer coatings. *Surf Coat Tech.* 2007;201(13):6122-30.
20. Silva LC, Libório MS, Lima LLF, Sousa RRM, Costa THC, Naeem M et al. Deposition of MoS₂-TiN multilayer films on 1045 steel to improve common rail injection system. *J Mater Eng Perform.* 2020;29(10):6740-7. <https://doi.org/10.1007/s11665-020-05156-3>.
21. Araújo AGF, Naeem M, Araújo LNM, Libório MS, Danelon MR, Monção RM et al. Duplex treatment with Hastelloy cage on AISI 5160 steel cutting tools. *Mater Sci Technol.* 2022;38(8):499-506.
22. Araújo FO, Sousa RRM, Costa JAP, Alves C Jr. Deposição de filme metálico em amostras de vidro em gaiola catódica. *Rev Bras Apl Vácuo.* 2008 [cited 2022 Aug 7];27(3):149-52. <http://www.sbvacu.org.br/rbav/index.php/rbav/article/view/442>.
23. Kertscher R, Moraes JM, Henke S, Allenstein AN, Gonçalves E, Silva RH et al. First results of cavitation erosion behavior of plasma nitrided niobium: surface modification. *Mater Res.* 2015 [cited 2022 Aug 16];18(6):1242-50. <http://www.scielo.br/j/mr/a/FTb5MJ7nJWbTjxvQJvHtH8B/?lang=en>.
24. Zhitomirsky VN, Grimberg I, Rapoport L, Travitzky NA, Boxman RL, Goldsmith S et al. Structure and mechanical properties of vacuum arc-deposited NbN coatings. *Thin Solid Films.* 1998;326(1-2):134-42.
25. Zhao H, Miao Q, Liang W, Yi J, Liu R, Xue L et al. A study on pre-treatment with rotation accelerated shot peening in multi-NbN films by double glow plasma surface metallurgy. *Surf Coat Tech.* 2021;405:126671.
26. Yang LX, Wang Y, Liu RJ, Liu HJ, Zeng CL, Fu C. Preparation and characterization of nanocrystalline β -Nb₂N coating on 430 ferritic stainless steel by disproportionation of Nb(IV) ions in molten salt. *Ceram Int.* 2020 [cited 2022 Aug 29];46(7):9319-27. <https://www.sciencedirect.com/science/article/pii/S0272884219336776>.
27. Cansever N, Danişman M, Kazmanli K. The effect of nitrogen pressure on cathodic arc deposited NbN thin films. *Surf Coat Tech.* 2008;202(24):5919-23.